PCP
PLANT & CELL PHYSIOLOGY

Special Focus Issue – Regular Paper

Dynamic Behavior of the *trans*-Golgi Network in Root Tissues of Arabidopsis Revealed by Super-Resolution Live Imaging

Tomohiro Uemura[1,*], Yasuyuki Suda[2], Takashi Ueda[1] and Akihiko Nakano[1,2]

[1]Department of Biological Sciences, Graduate School of Science, The University of Tokyo, Bunkyo-ku, Tokyo, 113-0033 Japan
[2]Live Cell Molecular Imaging Research Team, Extreme Photonics Research Group, RIKEN Center for Advanced Photonics, Wako, Saitama, 351-0198 Japan
*Corresponding author: E-mail, tuemura@biol.s.u-tokyo.ac.jp; Fax, +81-3-5841-7613.
(Received August 22, 2013; Accepted January 7, 2014)

The *trans*-Golgi network (TGN) is an important organelle for protein transport at the post-Golgi network, which functions as a sorting station that directs cargo proteins to a variety of destinations including post-Golgi compartments and the extracellular space. However, the functions and dynamics of the TGN in plant cells have not been well understood yet. To elucidate the dynamics of the plant TGN, we established transgenic plants expressing green fluorescent protein (GFP)–SYP43, the ortholog of Tlg2/syntaxin16, which is localized to the TGN in yeast and mammalian cells, under the control of the native promoter as a TGN marker. Observation by confocal laser scanning microscopy and super-resolution confocal live imaging microscopy revealed two types of TGN in Arabidopsis root: the GA-TGNs (Golgi-associated TGNs), located on the *trans*-side of the Golgi apparatus, and the GI-TGNs (Golgi-released independent TGNs), located away from the Golgi apparatus and behaving independently. The GI-TGNs is derived from a population of GA-TGNs by segregation, although the core of the GA-TGN remains even after the generation of the GI-TGN. We further found that the abundance of the GI-TGNs differs between observed tissues. Our results indicate that the dynamic features of the TGN in plant cells differ from those of animal and yeast cells.

Keywords: Arabidopsis • Live imaging • SNARE • TGN.

Abbreviations: BFA, brefeldin A; CLSM, confocal laser scanning microscopy; EE, early endosome; GA-TGN, Golgi-associated TGN; GFP, green fluorescent protein; GI-TGN, Golgi-released independent TGN; mRFP, monomeric red fluorescent protein; MS, Murashige and Skoog; PCR, partially coated reticulum; SCLIM, super-resolution confocal live imaging microscopy; SNARE, soluble *N*-ethylmaleimide-sensitive factor attachment protein receptor; TGN, *trans*-Golgi network; VHAa1, vacuolar ATPase subunit a1.

Introduction

In all eukaryotic cells, the post-Golgi organelles, such as the *trans*-Golgi network (TGN), endosomes, vacuoles and the plasma membrane, are connected by a network of membrane traffic (Glick and Nakano 2009, Saito and Ueda 2009). The TGN is a very important organelle for protein transport in the post-Golgi network. Initially, the TGN was defined as a specialized compartment on the *trans*-side of the Golgi apparatus that is responsible for delivering proteins to the plasma membrane, lysosomes and extracellular space from the Golgi apparatus (Roth et al. 1985, Griffiths and Simons 1986, Ladinsky et al. 1994). In animal cells, the TGN varies morphologically in different cell types. For example, the TGN is multilayered and extensive in cells that do not form large typical secretory granules such as Sertoli cells and spinal ganglion cells, but the TGN seems to be absent from cells forming very large secretory granules (Clermont et al. 1995). The TGN sorts various cargo proteins destined for the plasma membrane and endosomes (Keller and Simons 1997, Sannerud et al. 2003) and receives cargo from endosomal compartments (Pavelka et al. 1998, Shewan et al. 2003). Thus, the TGN represents a trafficking hub where the secretory and endocytic pathways merge. Indeed, it is still a matter for debate whether the TGN should be considered a Golgi subcompartment or an endocytic compartment in animal cells.

In plants, the TGN was initially considered a compartment structurally indistinguishable from the PCR (the partially coated reticulum), which was described as a tubulo-vesicular compartment with clathrin buds (Pesacreta and Lucas 1985, Staehelin and Moore 1995). However, many of the ramifying PCR networks were closely associated with the *trans*-side of the Golgi apparatus. They appeared to be equivalent to the animal TGN, which acts as a sorting station in the post-Golgi pathways, and thus it was proposed that the Golgi-associated PCR should

Plant Cell Physiol. 55(4): 694–703 (2014) doi:10.1093/pcp/pcu010, available online at www.pcp.oxfordjournals.org

called the TGN (Staehelin et al. 1990). In parallel, an experiment investigating the endocytic uptake of cationized ferritin showed that the PCR stood at an early stage in clathrin-mediated endocytosis (Staehelin et al. 1990). Consequently, the TGN and the PCR have been thought to serve different but overlapping functions in the exocytic and endocytic pathways, respectively, in plant cells.

Localization of Syntaxin of plant 41 (SYP41) and SYP61, members of SNARE (soluble *N*-ethylmaleimide-sensitive factor attachment protein receptor), VPS45 (a member of the Sec1/Munc18 family proteins) and VHAa1 (a subunit of V-ATPase) to the *trans*-most cisternae by immunogold labeling indicates that these molecules are good markers for the TGN in plants (Bassham et al. 2000, Sanderfoot et al. 2001, Dettmer et al. 2006). Live imaging techniques using fluorescent proteins such as GFP (green fluorescent protein), YFP (yellow fluorescent protein) and RFP (red fluorescent protein) enables visualization of the dynamics of the TGN in living cells. FM4-64, a lipophilic tracer dye for endocytosis, labels a compartment overlapping with VHAa1–GFP at an earlier time point than the compartment labeled by Rab5 GTPases (ARA6 and ARA7). This result suggested that the TGN can function as an early endosome (EE) (Dettmer et al. 2006). Recent findings by time-lapse imaging and immunogold electron microscopy support the role of the TGN as an EE. The plasma membrane-localized brassinosteroid receptor BRASSINOSTEROID INSENSITIVE1 and boron transporter BOR1 have been shown to pass through the TGN (Viotti et al. 2010). Therefore, in the plant field, it is plausible that the TGN also functions as an EE.

Arabidopsis mutants of TGN-localized proteins have revealed the physiological roles of the TGN. The SYP4 group consists of three genes: *SYP41*, *SYP42* and *SYP43*. SYP4s are the plant orthologs of Tlg2/Syntaxin16 (Qa-SNARE) that localizes to the TGN in yeast and animal cells. Mutant analyses revealed that SYP41, SYP42 and SYP43 possessed partly overlapping functions and that SYP42 and SYP43 play major roles in Col-0. The SYP4 proteins regulate secretory and vacuolar transport pathways and maintain the morphology of the Golgi apparatus and TGN. Consistent with a secretory role, SYP4 proteins are required for extracellular resistance to the host-adapted, virulent, powdery fungus *Golovinomyces orontii* (Uemura et al. 2012a). In addition to biotic stress, the TGN is associated with salt tolerance. Plants with double mutations in *SYP42* and *SYP43* and a single mutation in *SYP61*, whose product forms the SNARE complex with the SYP4 group in the TGN, exhibit growth arrest in a medium with a high concentration of NaCl (Zhu et al. 2002, Uemura et al. 2012b). Moreover, TNO1 (TGN-localized SYP41-interacting protein) is involved in vacuolar trafficking and salt tolerance (Kim and Bassham 2011). These results indicate that the TGN plays pivotal roles in biotic and abiotic stress resistance in plants.

However, knowledge about the TGN in plants is still limited, although a few studies have pointed out unique characters and dynamics of the plant TGN (Viotti et al. 2010, Choi et al. 2013). In the present study, we visualized the dynamic behavior of the TGN in several root tissues of Arabidopsis by using SCLIM (super-resolution confocal live imaging microscopy) that we developed (Matsuura-Tokita et al. 2006, Nakano and Luini 2010, Ito et al. 2012, Okamoto et al. 2012) and identified two types of TGN. One mainly locates adjacent to the Golgi apparatus and behaves together with it, and the other is separated from the Golgi apparatus. In addition, the behavior of the two types of TGN differs among tissues. These results indicate that the TGN is a dynamic organelle that functions as the hub of the post-Golgi network.

Results

Two types of the TGN exist in Arabidopsis root tissues

We have already reported that TGNs in which GFP-tagged SYP41 (GFP–SYP41) resided are clearly separated from but occasionally found very near the Golgi apparatus, when GFP–SYP41 is transiently expressed in protoplast cells from Arabidopsis cultured cells (Uemura et al. 2004). This result led us to speculate that the TGN might be defined as a separate compartment distinct from the Golgi apparatus in Arabidopsis cells. To exclude the possibility that overexpression by using the 35S promoter and transient expression in the protoplast affected the distribution of GFP–SYP41, we established transgenic Arabidopsis expressing GFP–SYP41, GFP–SYP42 and GYP–SYP43 under the control of their own promoters. SYP41, SYP42 and SYP43 have redundant physiological roles and co-localize on the TGN (Uemura et al. 2012a). Because the fluorescence signal of GFP–SYP43 is most prominent under CLSM (confocal laser scanning microscopy) as compared with GFP–SYP41 and GFP–SYP42, the transgenic expressing GFP–SYP43 was used for further observation to reveal the dynamics of the TGN in Arabidopsis. A population of GFP–SYP43 was observed on the plasma membrane in the division and elongation zone of root tissue. Although we cannot conclude whether or not this localization is due to overexpression, this does not affect observations for the TGN dynamics. First, we established transgenic Arabidopsis expressing GFP–SYP43 and ST–mRFP (cytoplasmic and transmembrane domains of sialyl transferase tagged with mRFP; a *trans*-Golgi marker) to examine the relationship between the TGN and the Golgi apparatus in living cells. Observation under CLSM demonstrated that TGNs labeled with GFP–SYP43 were associated with the *trans*-Golgi cisternae marked by ST–mRFP in cells of the root division zone (**Fig. 1A**). Interestingly, this result is inconsistent with that obtained from observations based on transient expression in protoplasts. Next, we observed the TGN structure of the cells in the root elongation zone. As with the root division zone, most of the TGNs labeled with GFP–SYP43 were associated with the *trans*-Golgi cisternae marked by ST–mRFP (**Fig. 1B**). However, we also found green fluorescence without red fluorescence (**Fig. 1B**, magnified image), suggesting that some TGNs exist independently from the Golgi apparatus, as in the case of

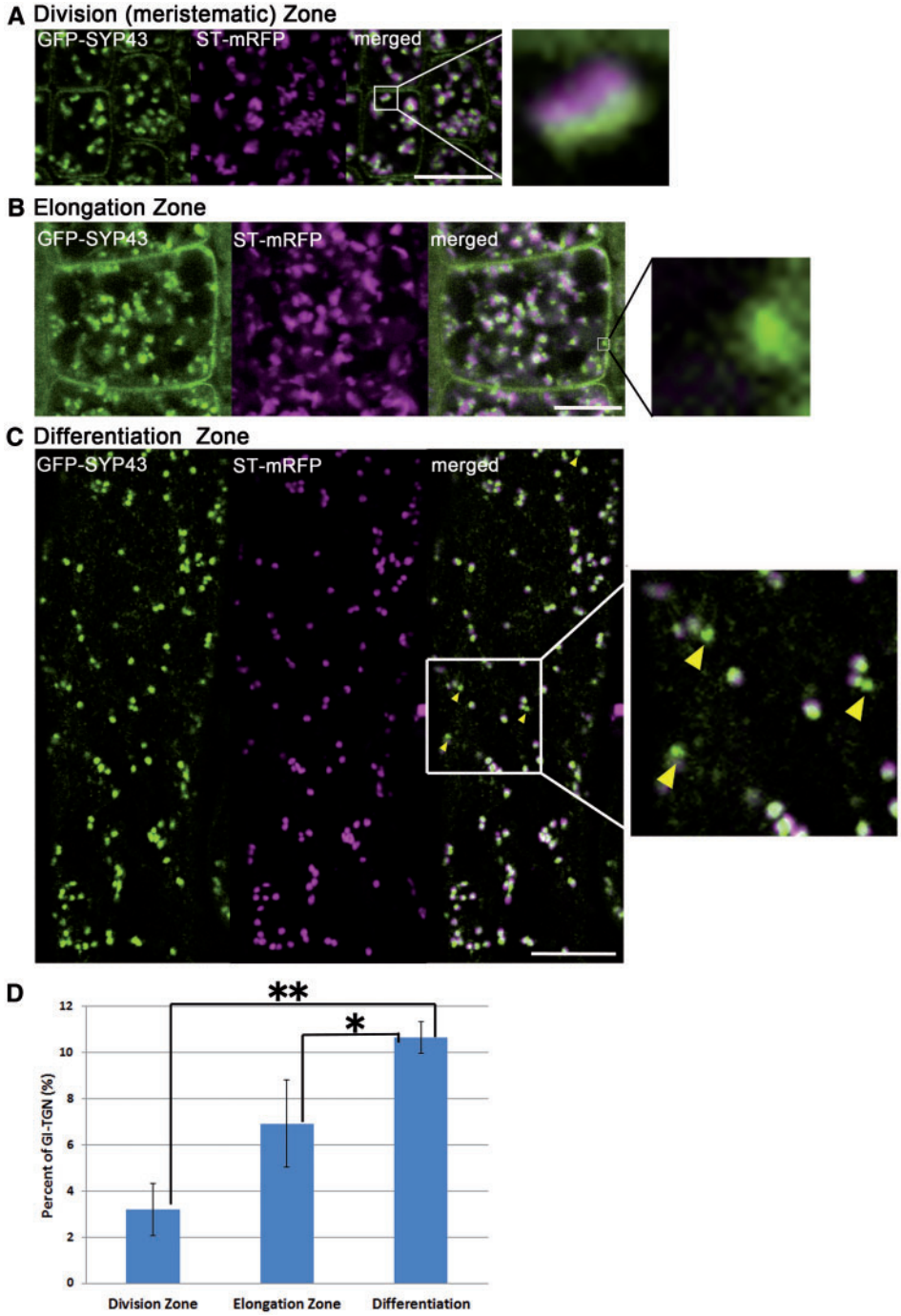

Fig. 1 Confocal images of Arabidopsis expressing GFP–SYP43 and ST–mRFP as TGN and Golgi markers, respectively. (A) In the root division zone. A magnified image representing the association between the TGN and Golgi apparatus (GA-TGN). (B) In the root elongation zone. A magnified image representing a TGN independent from the Golgi apparatus (GI-TGN). (C) In the root differentiation zone. Yellow arrowheads indicate the GI-TGN. Scale bars in (A–C) are 10 μm. (D) A graph representing the percentage of GI-TGNs in the division, elongation and differentiation zone of Arabidopsis root. A cell was picked from a confocal image, and dot-like signals with GFP fluorescence from GFP–SYP43 were counted. In total 3–4 independent images (147–360 TGNs) were analyzed. Error bars = SD. $^{*}P < 0.05$; $^{**}P < 0.01$.

protoplast cells. Further observation in the root differential zone revealed that TGNs independent from the Golgi apparatus were easily observable (**Fig. 1C**, arrowheads). Here, we designate the TGN associated with the Golgi apparatus and the TGN independent from the Golgi apparatus as the Golgi-associated TGN (GA-TGN) and the Golgi-released independent TGN (GI-TGN), respectively.

To characterize the GI-TGNs, the number of GI-TGNs in 3–4 cells of each division, elongation and differentiation zone was counted for quantitative analysis. As shown in **Fig. 1D**, the

number of GI-TGNs in the differentiation zone was clearly larger than in the division and elongation zones. GI-TGNs were rarely observed in the division zone. The ratio of GI-TGNs in the differentiation zone was over three times higher than that of the division zone.

Next, to investigate the possibility that a *trans*-Golgi cisterna labeled by ST–mRFP might behave independently from a *cis*-Golgi cisterna and that the GI-TGNs were observed as the result of dynamic behavior of the GFP–SYP43-labeled TGN in elongation and differentiation zones, we generated transgenic plants expressing GFP–ERD2 (ER retention defective 2 tagged with GFP; a *cis*-Golgi marker) and ST–mRFP (the *trans*-Golgi marker), and those expressing GFP–SYP43 and VHAa1–mRFP (another TGN marker). CLSM observation of the transgenic plants expressing ERD2–GFP and ST–mRFP showed that the fluorescence of GFP and mRFP was almost completely co-localized in the division, elongation and differentiation zones of root. Punctate structures with partial overlapping of GFP and mRFP fluorescence were often seen; however, non-overlapping fluorescence patterns were not observed in any types of cells (**Fig. 2A**). These results indicate that the GI-TGN actually exists separated from the Golgi apparatus, while the *cis*- and *trans*-cisternae of the Golgi apparatus behave together at all times.

Then, we examined the transgenic line expressing GFP–SYP43 and VHAa1–mRFP. GFP–SYP43 and VHAa1–mRFP were almost completely co-localized in the division, elongation and differentiation zones of root, and no fluorescence signal from GFP alone or mRFP alone was observed (**Fig. 2B**). These results suggest that the feature of GI-TGNs described in **Fig. 1** is not specific to GFP–SYP43 but represents the nature of the TGN itself in the root cells.

Taken together, we conclude that Arabidopsis root contains two types of TGN: the GA-TGN, located on the *trans*-side of the Golgi apparatus, and the GI-TGN, which does not lie adjacent to the Golgi apparatus and behaves independently. GI-TGN was detected more frequently in the differentiation zone of root.

Characterization of the GA-TGN and GI-TGN by BFA treatment

To characterize the GA-TGN and GI-TGN, we investigated the response to brefeldin A (BFA) of the GA-TGN and GI-TGN in the division, elongation and differentiation zones of the root. BFA, an antibiotic compound produced by fungi, is known as a potent inhibitor of guanine nucleotide exchange factors for ARF GTPases (McCloud et al. 1995, Chardin and McCormick 1999). BFA treatment leads to TGN and endosome aggregation in Arabidopsis root and cotyledon cells (Robinson et al. 2008, Uemura and Nakano 2013). When Arabidopsis root expressing GFP–SYP43 and ST–mRFP was treated with BFA for 2 h, cells in the division zone showed TGNs labeled with GFP–SYP43 (almost all GA-TGNs) aggregating at the center of the BFA body. In the same cells, Golgi apparatus labeled with ST–mRFP accumulated at the periphery of the TGN accumulation. Quantitative analysis of GFP and mRFP fluorescence clearly

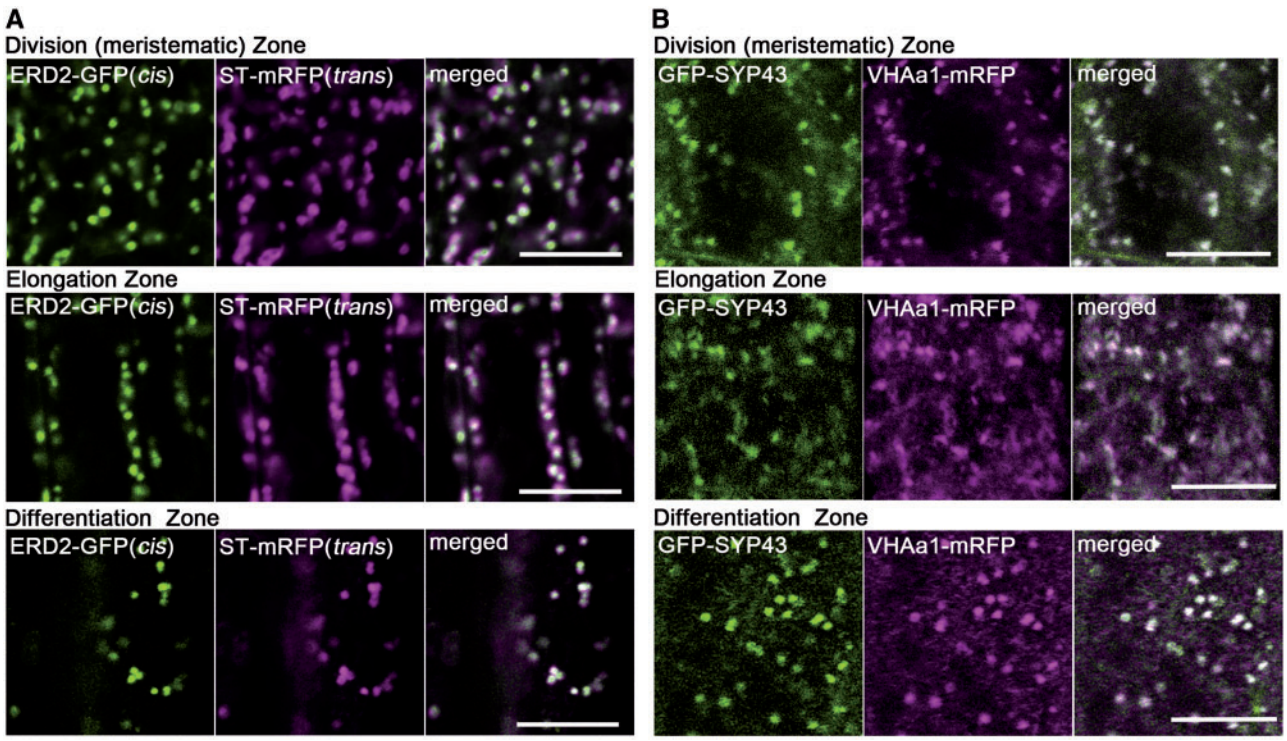

Fig. 2 Relationship between *cis*-Golgi and *trans*-Golgi cisternae and between TGN labeled with different markers. (A) Confocal images of Arabidopsis expressing ERD2–GFP and ST–mRFP in the division, elongation and differentiation zones of the root. (B) Confocal images of Arabidopsis expressing GFP–SYP43 and VHAa1–mRFP in the division, elongation and differentiation zones of root. Scale bars are 10 μm.

demonstrated that the TGN was centrally located in the BFA body (Fig. 3A). Similar results were obtained from observations in the elongation and differentiation zones of root (Fig. 3B, C). Because the GI-TGN, which is marked by an independent GFP signal and not associated with ST–mRFP, was not observed upon BFA treatment even in the differentiation zone, we inferred that the GI-TGN was also contained in the BFA body. These results suggest that the response of the GI-TGN to BFA was similar to that of the GA-TGN in Arabidopsis root, at least under the experimental conditions we employed in this study.

Characterization of the GA-TGN and GI-TGN by SCLIM

Next, to characterize the difference between the GA-TGN and GI-TGN in more detail, the relationships between the Golgi apparatus and the GA- and GI-TGN were investigated using SCLIM, which enables two-color observation with extremely high speed and sensitivity. The GFP–SYP43/ST–mRFP-expressing plant was observed by SCLIM with optical slices 0.1 μm apart in the *z*-axis, and 21 images were reconstructed into 3D with deconvolution to achieve high spatial resolution. In the division zone, the Golgi apparatus labeled by ST–mRFP was observed as a flat donut-like structure, and the GA-TGN labeled by GFP–SYP43 was clearly associated with and located at the *trans*-side end of the Golgi apparatus. The surface of the TGN on the opposite side of the Golgi apparatus seemed to be an irregular structure (Fig. 4A). In the differentiation zone, GI-TGNs were easily observed. Unlike the GA-TGN structure, GI-TGNs, which were obviously not associated with the Golgi apparatus, had a smooth and round shape (Fig. 4B, white arrowheads). In addition, we observed occasional association of GI-TGNs and GA-TGNs (Fig. 4B, yellow arrowheads). These results imply that GI-TGNs exchange materials with GA-TGNs, or GI-TGNs could be generated by maturation from the GA-TGNs. Some small puncta showed only GFP fluorescence without mRFP, but these might be due to background noises.

GI-TGNs were generated by GA-TGNs dissociated from the Golgi apparatus

Here, we address the question of whether GI-TGNs were derived from GA-TGNs or generated de novo. To answer this question, a transgenic plants expressing GFP–SYP43 and ST–mRFP was observed by 3D time-lapse imaging (4D imaging) of SCLIM. From a GA-TGN, whose action was linked to that of the Golgi apparatus (Fig. 5A, yellow arrowheads, time point from

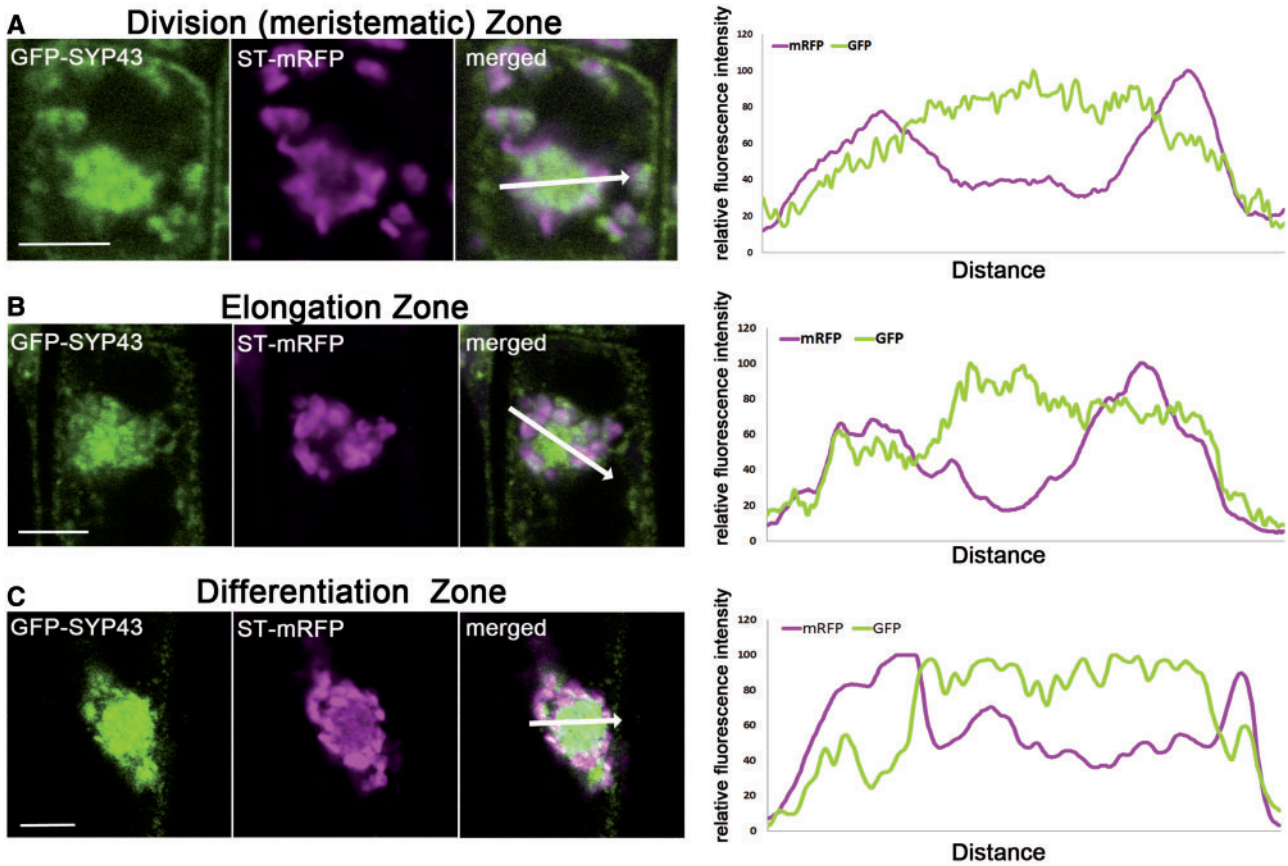

Fig. 3 Effects of BFA on the *trans*-Golgi cisterna and TGN. Confocal images of Arabidopsis expressing GFP–SYP43 and ST–mRFP after BFA treatment (50 μM, 2 h) are shown. (A) In the root division zone. (B) In the root elongation zone. (C) In the root differentiation zone. Each graph represents the fluorescence intensities of GFP and mRFP along the arrows in the merged image. Scale bars are 10 μm.

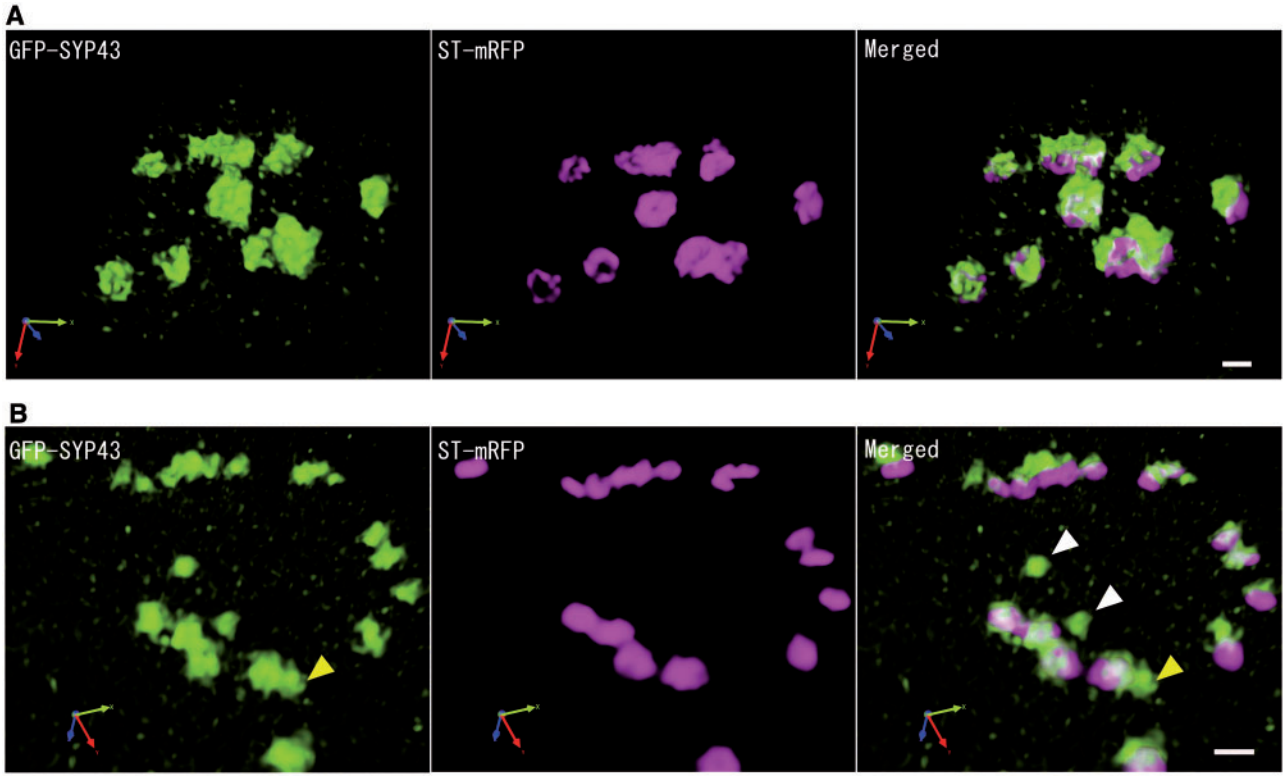

Fig. 4 High-resolution 3D images of GA-TGNs and GI-TGNs. Arabidopsis expressing GFP–SYP43 and ST–mRFP was observed by SCLIM with optical slices 0.1 μm apart in the z-axis. 3D images were reconstructed and deconvolved. (A) In a cell of the division zone, GA-TGNs were mainly observed. (B) In a cell of the differentiation zone, GI-TGNs were also observed. Yellow arrowheads show the GI-TGN interaction with the GA-TGN. White arrowheads indicate GI-TGNs behaving independently. Scale bars are 1 μm.

0.0 to 13.2 s; **Supplementary Movie S1**), a new GI-TGN was generated (**Fig. 5A**, red arrowheads, time point of 19.8 s; **Supplementary Movie S1**). Interestingly, a portion of the GA-TGN remained beside the Golgi apparatus (**Fig. 5A**, orange arrowhead, time point 19.8 s, yellow arrowhead; **Supplementary Movie S1**). After that, the remaining GA-TGNs and the Golgi apparatus moved together (**Fig. 5A**, time point from 26.4–46.2 s; **Supplementary Movie S1**). **Fig. 5B** show enlarged images of the same event indicating that a GI-TGN forms by budding from a pre-existing GA-TGN. Once the GI-TGN was generated, it moved around freely, independently from the Golgi apparatus (**Fig. 5B**). We also observed that two GI-TGNs interacted with each other, moved together and eventually separated again (**Fig. 5A**, white arrowheads; **Supplementary Movie S1**). Another observation of the generation of GI-TGNs was demonstrated in **Fig. 5C** and **D**. These results suggest that GI-TGNs are derived from a population of GA-TGNs by segregation and that they can communicate with each other.

Next, the behavior of a GA-TGN, after giving rise to a GI-TGN, was examined in detail by 4D imaging. As shown in **Fig. 6A**, we identified the moment when a GI-TGN was generated from a GA-TGN (time points from 17.7 to 20.65 s, white arrowheads). A homotypic interaction of two GA-TGNs was observed earlier (**Fig. 6A**, red arrowheads). Then, the dynamics of GA-TGNs after segregation (**Fig. 6A**, time point 20.65 s, white open square) was continuously observed (**Fig. 6B**; **Supplementary Movie S2**). Time-lapse images indicated that the intensity of GFP fluorescence gradually increased whereas that of mRFP decreased (**Fig. 6B**). For quantitative analysis, we compared the total fluorescent intensity of GFP and mRFP in the images shown in **Fig. 6B** and found that the intensity of the GFP fluorescence from GA-TGN after 120 s of segregation was almost 1.5 times higher than that of the GA-TGN soon after the GI-TGN was generated (**Fig. 6C**). The decreasing intensity of mRFP from the Golgi apparatus could have resulted from photobleaching. These results imply that the core of the GA-TGN remains even after the generation of the GI-TGN and that the GA-TGN is re-organized by recapturing TGN proteins.

Discussion

The TGN is an organelle diversified in a cell type-dependent manner in plants

Like in animal and fungal cells, the TGN used to be considered a part of the Golgi apparatus in plant cells (Staehelin and Moore 1995). However, this concept is changing recently based on several findings. Live-cell imaging with spinning disk confocal microscopy (Viotti et al. 2010) has shown that the TGN/EE

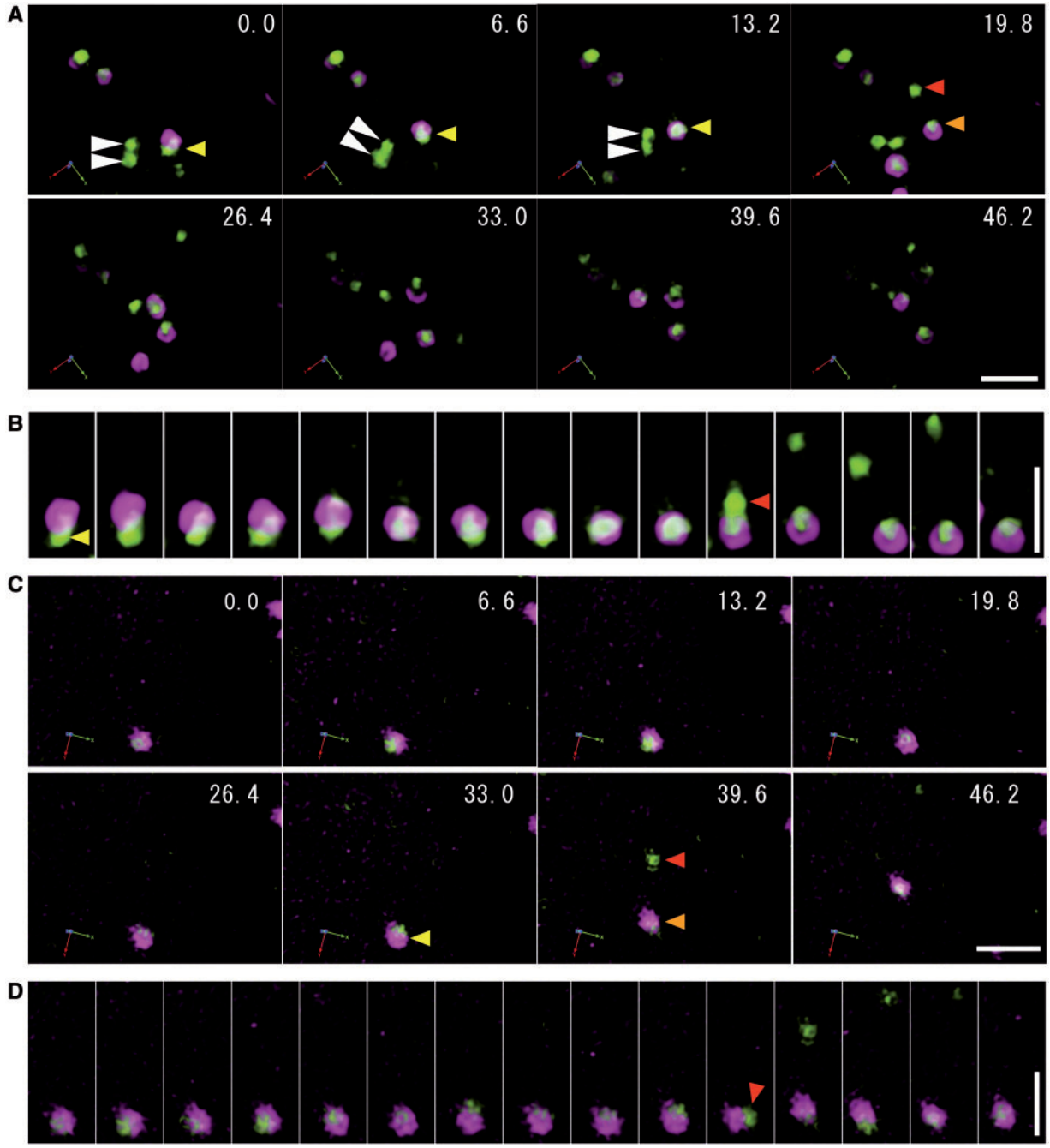

Fig. 5 The GI-TGN is derived from the GA-TGN by dissociation. (A) 4D imaging of GA-TGNs and GI-TGNs. Arabidopsis expressing GFP–SYP43 and ST–mRFP was observed by SCLIM with optical slices 0.1 μm apart on the *x*-axis. Fifteen images were taken for 1 s, and 3D images consisting of 11 images were reconstructed and deconvolved. Fifty time points were continuously observed as 4D imaging. The red arrow indicates GI-TGN dissociation from the GA-TGN (yellow arrowheads). (B) Magnified and detailed images of GI-TGNs shown in (A). Images are lined up every 1.2 s from left to right. (C) 4D imaging of GA-TGNs and GI-TGNs. Arabidopsis expressing GFP–SYP43 and ST–mRFP was observed by SCLIM with optical slices 0.25 μm apart on the *z*-axis. Eight images were taken for 1 s, and 3D images consisting of 11 images were reconstructed and deconvolved. Fifty time points were continuously observed as 4D imaging. The red arrow indicates GI-TGN dissociation from the GA-TGN (yellow arrowhead). (D) Magnified and detailed images of GI-TGNs shown in (C). Images are lined up every 3.3 s from left to right. Scale bars are 3 μm.

behaves as a highly mobile and independent organelle, which transiently becomes closely associated with the Golgi apparatus in Arabidopsis hypocotyl cells. In this report, homotypic association and dissociation of the TGN/EE were also observed. Another line of studies by electron microscopy and tomography (Staehelin and Kang, 2008, Kang et al. 2011) demonstrated that RabA4b-labeled TGN compartments were closely associated with the Golgi apparatus and that this

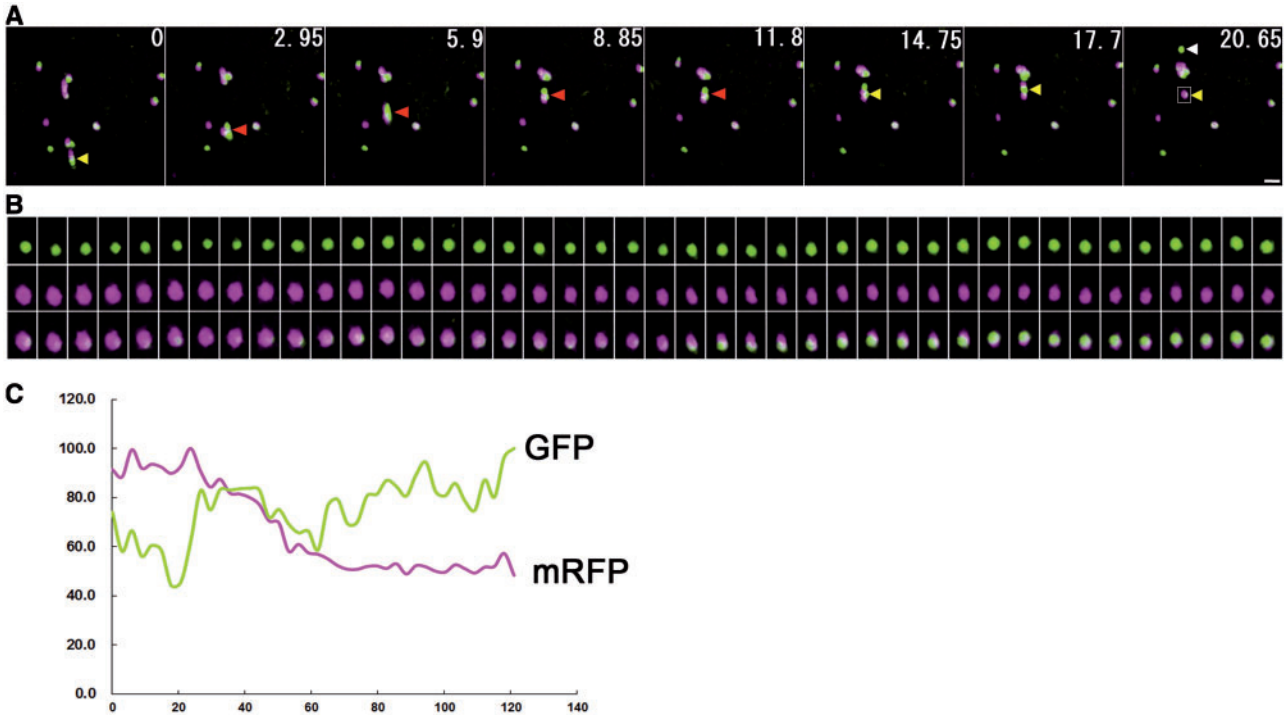

Fig. 6 The GA-TGN remained as a core after derivation of the GI-TGN from the GA-TGN by dissociation. Arabidopsis expressing GFP–SYP43 and ST–mRFP was observed by SCLIM with optical slices 0.25 μm apart on the *z*-axis. Eight images were taken for 1 s, and 3D images consisting of 21 images were reconstructed and deconvolved. Thirty time points were continuously observed as 4D imaging. (A) 4D imaging of GA-TGNs and GI-TGNs. A white arrow indicates GI-TGN dissociation from the GA-TGN (yellow arrowheads). Red arrows indicate homotypic interaction of GA-TGNs. (B) Magnified and detailed 4D images of the white open square shown in (A). The images represent the dynamics of GA-TGNs every 1.45 s just after 20.65 s shown in (A). (C) Total fluorescence intensity of GFP and mRFP in the images shown in (B). Scale bar is 2 μm.

Golgi-associated TGN was formed from a *trans*-Golgi cisterna in Arabidopsis root meristem cells, with a 30–35% reduction in cisternal membranes. In addition, the free TGN compartments were defined as cisternae that had detached from the Golgi cisternae to become an independent organelle. In the present study, we have found two types of TGN in Arabidopsis root: the GA-TGN, which is located on the *trans*-side of the Golgi apparatus, and the GI-TGN, which is not located adjacent to the Golgi apparatus and behaves independently. The frequency of GI-TGNs is high in the differentiation zone of the root. GI-TGNs are derived from a population of GA-TGNs by segregation. From these features, we consider that the Golgi-associated TGN of Kang et al. (2011) is equivalent to the GA-TGN in the present study.

The GI-TGN, on the other hand, is rarely observed in Arabidopsis root meristem cells (**Fig. 1**), but Kang et al. (2011) identified free TGNs in these cells. This may be due to the limitation of detecting GI-TGNs by fluorescent live imaging as compared with electron microscopy. Nevertheless, our results clearly support the recent idea that the TGN could be an independent organelle distinct from the Golgi apparatus.

This report is the first to characterize and compare the TGN in different cells by super-resolution imaging, and we have found that the patterns of characteristics of the TGN differ among tissues and cell types. In tobacco (*Nicotiana tabacum*) BY-2 cells, the secretory vesicle cluster, which is derived from the TGN and can be labeled with secretory carrier membrane protein 2, moves within the cell and fuses with the plasma membrane (Toyooka et al. 2009). The secretory vesicle cluster is likely to be equivalent to the GI-TGN (present study) and free TGN (Kang et al. 2011).

At this time, we do not have an answer as to why the GI-TGN increases in the differentiation zone. The cells of the differentiation zone have a larger volume than those of the division zone. The cell volume might be a key factor in the generation of the GI-TGN. In fact, the TGN that is unassociated with the Golgi apparatus is easily observed in several cells such as the epidermal cells of the hypocotyl (Viotti et al. 2010). Although the question remains as to whether these are equivalent or not, further analyses will provide new insights into the TGN and reveal the physiological function of the GI-TGN.

The maturation of the GA-TGN after delivery of the GI-TGN

In the cisternal maturation model, a new cisterna is formed at the *cis*-side of the stack by endoplasmic reticulum-derived carriers and progresses from the *cis*- to the *trans*-Golgi cisterna as it matures (Glick and Nakano 2009, Nakano and Luini 2010). Electron microscopic observation has suggested that the GA-TGN is generated from the *trans*-most Golgi cisterna by

maturation and that the GA-TGN has lost its association with the cisternal membrane and separated from the Golgi apparatus as an independent organelle (Kang et al. 2011). Our observation by SCLIM has demonstrated that the GA-TGN, just after releasing the GI-TGN, re-matures by capturing TGN proteins. There are many possible explanations for this phenomenon. Newly synthesized TGN proteins might be transported to the GA-TGN in a de novo pathway or the maturation from *trans*-Golgi cisternae to GA-TGNs could accelerate. Another possibility is that TGN proteins, which localized on a distinct GI-TGN, might be recruited to a newly generated GA-TGN. In fact, homotypic and heterotypic associations between the two types of TGN are often observed (**Fig. 4**). However, as such an association was not observed during the maturation of the GA-TGN (**Fig. 6**), small transport vesicles budding from the GI-TGN and fusing with the GA-TGN might contribute to recycling, rather than the direct interaction between the GA-TGN and GI-TGN. In any case, we propose that the maturation of the GA-TGN continues after biogenesis of the GI-TGN.

Questions to be resolved

When we realized the presence of Golgi-independent TGNs in plants and decided to begin to study their characteristics (Uemura et al. 2004), TGN-related resources were very limited. Now many TGN-localized proteins have been identified and the physiological roles of the TGN have been proposed. The ECHIDNA (ECH) protein of *Arabidopsis thaliana* is an ortholog of the yeast Tlg2p-vesicle protein 23, which was identified in purified Tlg2-vesicles. ECH is mainly localized on the TGN, and a mutation in ECH (*ech*) results in severely perturbed cell elongation and defects in the TGN structure (Gendre et al. 2011). SYP61 (Qc-SNARE), which interacts with the SYP4 group, is also widely accepted as a TGN marker (Sanderfoot et al. 2001, Uemura et al. 2004). To understand the differentiated roles of the GA-TGN and GI-TGN, it will be essential to investigate the detailed suborganellar localizations of TGN markers (such as SYP4, SYP6, VHAa1 and ECH) simultaneously. A combination of live imaging and genetic analysis using mutants will reveal the mechanism which maintains the morphology and regulates the functions of TGN, and lead to a clearer definition of the GA-TGN and GI-TGN.

Materials and Methods

Plant materials and plasmids

Plants expressing GFP–SYP43 or ST–mRFP have already been reported (Uemura et al. 2012a), and plants that express VHAa1–mRFP were gifts from Karin Schumacher (University of Heidelberg, Germany). The plants expressing GFP–SYP43/ST–mRFP or GFP–SYP43/VHAa1–mRFP were generated by crossing. Seeds were sterilized in 1% sodium hypochlorite and 0.05% Tween, rinsed with sterile distilled water three times and sown on Murashige and Skoog (MS) medium (pH 6.3) supplemented with 2% sucrose, 0.3% phytagel and 1× Gamborg's vitamins. The plants were incubated for 1 d at 4°C in the dark and cultivated at 23°C under continuous light. We observed cortex cells in the division and elongation zone and epidermal cells (first layer) in the differentiation zone of transgenic plants (5 d after germination).

Confocal microscopy

For 2D observation, a confocal laser scanning microscope, LSM780 (Carl Zeiss), was used. For high-resolution 3D or 4D imaging, SCLIM was employed. In the SCLIM system that we developed (Matsuura-Tokita et al. 2006, Nakano and Luini, 2010, Ito et al. 2012, Okamoto et al. 2012), an Olympus IX-70 microscope was equipped with an Olympus oil-immersion lens UPlanSApo (×100, NA 1.4), a custom-made super-low-noise and high-speed confocal scanner (Yokogawa Electric), a custom-made spectroscopic filter system, custom-made cooled image intensifiers (Hamamatsu Photonics), and high-speed and high-sensitivity EM-CCD cameras (Hamamatsu Photonics). Data were oversampled and subjected to a deconvolution analysis with Volocity (PerkinElmer) by using the point-spread function optimized for the Yokogawa spinning disk confocal system.

Drug treatment

Five- to seven-day-old seedlings were incubated in 1 ml of MS medium with 50 μM BFA (Sigma) for 2 h. After treatment, the fluorescence was observed with CLSM (LSM780) as described above.

Supplementary data

Supplementary data are available at PCP online.

Funding

This work was supported by the Ministry of Education, Culture, Sports, Science and Technology of Japan Grants-in-Aid for Scientific Research to A.N. (No. 25221103) and to T.U. (Nos. 25840100 and 25120706); RIKEN [the Extreme Photonics and the Cellular Systems Biology Projects]; The Sumitomo Foundation [Grant for Basic Science Research Projects].

Acknowledgments

We thank K. Schumacher for sharing materials. We also thank members of the Nakano Laboratory for valuable discussions.

Disclosures

The authors have no conflicts of interest to declare.

PCP PLANT & CELL PHYSIOLOGY

References

Bassham, D.C., Sanderfoot, A.A., Kovaleva, V., Zheng, H. and Raikhel, N.V. (2000) AtVPS45 complex formation at the trans-Golgi network. *Mol. Biol. Cell* 11: 2251–2265.

Chardin, P. and McCormick, F. (1999) Brefeldin A: the advantage of being uncompetitive. *Cell* 97: 153–155.

Choi, S.W., Tamaki, T., Ebine, K., Uemura, T., Ueda, T. and Nakano, A. (2013) RABA members act in distinct steps of subcellular trafficking of the FLAGELLIN SENSING2 receptor. *Plant Cell* 25: 1174–1187.

Clermont, Y., Rambourg, A. and Hermo, L. (1995) Trans-Golgi network (TGN) of different cell types: three-dimensional structural characteristics and variability. *Anat. Rec.* 242: 289–301.

Dettmer, J., Hong-Hermesdorf, A., Stierhof, Y.D. and Schumacher, K. (2006) Vacuolar H+-ATPase activity is required for endocytic and secretory trafficking in Arabidopsis. *Plant Cell* 18: 715–730.

Gendre, D., Oh, J., Boutte, Y., Best, J.G., Samuels, L., Nilsson, R. et al. (2011) Conserved Arabidopsis ECHIDNA protein mediates *trans*-Golgi-network trafficking and cell elongation. *Proc. Natl Acad. Sci. USA* 108: 8048–8053.

Glick, B.S. and Nakano, A. (2009) Membrane traffic within the Golgi apparatus. *Annu. Rev. Cell Dev. Biol.* 25: 113–132.

Griffiths, G. and Simons, K. (1986) The trans Golgi network: sorting at the exit site of the Golgi complex. *Science* 234: 438–443.

Ito, Y., Uemura, T., Shoda, K., Fujimoto, M., Ueda, T. and Nakano, A. (2012) *cis*-Golgi proteins accumulate near the ER exit sites and act as the scaffold for Golgi regeneration after brefeldin A treatment in tobacco BY-2 cells. *Mol. Biol. Cell* 23: 3203–3214.

Kang, B.H., Nielsen, E., Preuss, M.L., Mastronarde, D. and Staehelin, L.A. (2011) Electron tomography of RabA4b- and PI-4Kβ1-labeled *trans* Golgi network compartments in *Arabidopsis*. *Traffic* 12: 313–329.

Keller, P. and Simons, K. (1997) Post-Golgi biosynthetic trafficking. *J. Cell Sci.* 110: 3001–3009.

Kim, S.J. and Bassham, D.C. (2011) TNO1 is involved in salt tolerance and vacuolar trafficking in Arabidopsis. *Plant Physiol.* 156: 514–526.

Ladinsky, M.S., Kremer, J.R., Furcinitti, P.S., McIntosh, J.R. and Howell, K.E. (1994) HVEM tomography of the trans-Golgi network: structural insights and identification of a lace-like vesicle coat. *J. Cell Biol.* 127: 29–38.

Matsuura-Tokita, K., Takeuchi, M., Ichihara, A., Mikuriya, K. and Nakano, A. (2006) Live imaging of yeast Golgi cisternal maturation. *Nature* 441: 1007–1010.

McCloud, T.G., Burns, M.P., Majadly, F.D., Muschik, G.M., Miller, D.A., Poole, K.K. et al. (1995) Production of brefeldin-A. *J. Ind. Microbiol.* 15: 5–9.

Nakano, A. and Luini, A. (2010) Passage through the Golgi. *Curr. Opin. Cell Biol.* 22: 471–478.

Okamoto, M., Kurokawa, K., Matsuura-Tokita, K., Saito, C., Hirata, R. and Nakano, A. (2012) High-curvature domains of the ER are important for the organization of ER exit sites in *Saccharomyces cerevisiae*. *J. Cell Sci.* 125: 3412–3420.

Pavelka, M., Ellinger, A., Debbage, P., Loewe, C., Vetterlein, M. and Roth, J. (1998) Endocytic routes to the Golgi apparatus. *Histochem. Cell Biol.* 109: 555–570.

Pesacreta, T.C. and Lucas, W.J. (1985) Presence of a partially-coated reticulum in angiosperms. *Protoplasma* 125: 173–184.

Robinson, D.G., Jiang, L. and Schumacher, K. (2008) The endosomal system of plants: charting new and familiar territories. *Plant Physiol.* 147: 1482–1492.

Roth, J., Taatjes, D.J., Lucocq, J.M., Weinstein, J. and Paulson, J.C. (1985) Demonstration of an extensive trans-tubular network continuous with the Golgi apparatus stack that may function in glycosylation. *Cell* 43: 287–295.

Saito, C. and Ueda, T. (2009) Functions of RAB and SNARE proteins in plant life. *Int. Rev. Cell Mol. Biol.* 274: 183–233.

Sanderfoot, A.A., Kovaleva, V., Bassham, D.C. and Raikhel, N.V. (2001) Interactions between syntaxins identify at least five SNARE complexes within the Golgi/prevacuolar system of the Arabidopsis cell. *Mol. Biol. Cell* 12: 3733–3743.

Sannerud, R., Saraste, J. and Goud, B. (2003) Retrograde traffic in the biosynthetic–secretory route: pathways and machinery. *Curr. Opin. Cell Biol.* 15: 438–445.

Shewan, A.M., van Dam, E.M., Martin, S., Luen, T.B., Hong, W., Bryant, N.J. et al. (2003) GLUT4 recycles via a trans-Golgi network (TGN) subdomain enriched in Syntaxins 6 and 16 but not TGN38: involvement of an acidic targeting motif. *Mol. Biol. Cell* 14: 973–986.

Staehelin, L.A., Giddings, T.H., Kiss, J.Z. and Sack, F.D. (1990) Macromolecular differentiation of Golgi stacks in root-tips of Arabidopsis and Nicotiana seedlings as visualized in high-pressure frozen and freeze-substituted samples. *Protoplasma* 157: 75–91.

Staehelin, L.A. and Kang, B.H. (2008) Nanoscale architecture of endoplasmic reticulum export sites and of Golgi membranes as determined by electron tomography. *Plant Physiol.* 147: 1454–1468.

Staehelin, L.A. and Moore, I. (1995) The plant Golgi-apparatus—structure, functional-organization and trafficking mechanisms. *Annu. Rev. Plant Physiol.* 46: 261–288.

Toyooka, K., Goto, Y., Asatsuma, S., Koizumi, M., Mitsui, T. and Matsuoka, K. (2009) A mobile secretory vesicle cluster involved in mass transport from the Golgi to the plant cell exterior. *Plant Cell* 21: 1212–1229.

Uemura, T., Kim, H., Saito, C., Ebine, K., Ueda, T., Schulze-Lefert, P. and Nakano, A. (2012a) Qa-SNAREs localized to the trans-Golgi network regulate multiple transport pathways and extracellular disease resistance in plants. *Proc. Natl Acad. Sci. USA* 109: 1784–1789.

Uemura, T. and Nakano, A. (2013) Plant TGNs: dynamics and physiological functions. *Histochem. Cell Biol.* 140: 341–345.

Uemura, T., Ueda, T. and Nakano, A. (2012b) The physiological role of SYP4 in the salinity and osmotic stress tolerances. *Plant Signal. Behav.* 7: 1118–1120.

Uemura, T., Ueda, T., Ohniwa, R.L., Nakano, A., Takeyasu, K. and Sato, M.H. (2004) Systematic analysis of SNARE molecules in Arabidopsis: dissection of the post-Golgi network in plant cells. *Cell Struct. Funct.* 29: 49–65.

Viotti, C., Bubeck, J., Stierhof, Y.D., Krebs, M., Langhans, M., van den Berg, W. et al. (2010) Endocytic and secretory traffic in Arabidopsis merge in the trans-Golgi network/early endosome, an independent and highly dynamic organelle. *Plant Cell* 22: 1344–1357.

Zhu, J., Gong, Z., Zhang, C., Song, C.P., Damsz, B., Inan, G. et al. (2002) OSM1/SYP61: a syntaxin protein in Arabidopsis controls abscisic acid-mediated and non-abscisic acid-mediated responses to abiotic stress. *Plant Cell* 14: 3009–3028.